Phase-Doppler interferometry with probe-to-droplet size ratios less than unity. II. Application of the technique

Peter A. Strakey, Douglas G. Talley, Subra V. Sankar, and Will D. Bachalo

Practical limitations associated with the use of small probe volumes with respect to the droplet size that is being measured by the phase-Doppler interferometry technique are discussed. An intensity-validation scheme and corresponding probe volume correction factor have been developed that reject trajectory errors and account for the rejections in calculation of the probe cross-sectional area. The intensity-validation scheme also provides a tractable method of setting the photomultiplier tube gain and laser power. Volume flux measurements in dilute sprays have shown a significant improvement over those made by standard phase-Doppler interferometry techniques at small beam waist/droplet size ratios.

OCIS codes: 120.3180, 120.4640, 120.5050.

1. Introduction

Phase Doppler interferometry (PDI), which is a single-particle counting technique, requires that the probe volume, defined by the laser beam waist and the spatial filter, be made small enough to ensure that only one droplet is present in the probe volume at any given time. For sprays in which both the droplet number density and droplet sizes are relatively large, the laser beam waist must often times be made smaller than the maximum droplet size that is being measured. Whereas there is no fundamental restriction on this approach, there are several issues that arise when one is measuring droplets larger than the probe diameter. One challenging problem with the PDI technique when the droplet size becomes comparable to or larger than the probe diameter has been referred to as trajectory error. This is the issue that has also received the most attention in the literature in the past several years.[1] In Ref. 2, the predecessor to this paper, it was demonstrated that accurate size measurements can be made at probe-to-droplet size ratios, D_w/D, as small as 0.17. It was also demonstrated that trajectory errors caused by reflective contributions to the scattered-light signal can be eliminated with a combination of a three-detector phase-ratio criterion and an intensity-validation technique. The phase-ratio validation criterion with a noninteger detector separation ratio has been shown to eliminate erroneous reporting of large droplets as smaller droplets. The intensity-validation criterion prevents small droplets from being measured as much larger droplets. It has also been shown that intensity validation provides a simple and robust method of measuring the probe cross-sectional area, which is necessary for calculation of the spray mass flux.

Along with trajectory errors, there are a number of other potential problems that arise when the probe diameter and the slit size are made much smaller than the droplet size of interest. Some of the issues that must be addressed include

(i) Instrument limitations for short Doppler burst times,
(ii) Signal visibility effects,
(iii) Probe volume correction factors appropriate for large droplet-to-probe size ratios.
(iv) Phase variance as droplets pass through the probe volume.

We address each of these issues in the following sections with the intent of providing a sound methodology for applying the small probe volume (with respect to the droplet size) PDI technique in realistic spray environments.

P. A. Strakey (peter_strakey@ple.af.mil) and D. G. Talley are with the U.S. Air Force Research Laboratory, AFRL/PRSA, 10 East Saturn Boulevard, Edwards Air Force Base, California 93524. S. V. Sankar and W. D. Bachalo are consultants at 14660 Saltamontes Way, Los Altos Hills, California 94022.

Received 5 November 1999; revised manuscript received 4 April 2000.

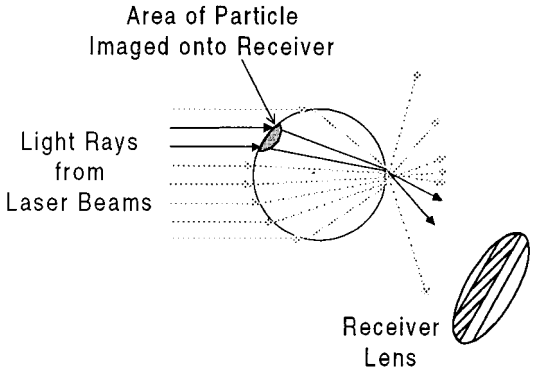

Fig. 1. Illustration of ray paths reaching the receiver lens.

2. Transit Time Limitations

Without its being possible to measure multiple particles in the probe volume, it is necessary that the size of the probe volume be reduced until the probability of finding multiple particles within the probe volume is negligibly small. In effect, the probe volume can theoretically be made much smaller than the size of the droplet that is being measured, as was demonstrated by Haugen *et al.*[3] For sizing nonabsorbing droplets, the forward-scattering region is advantageous in maximizing light-scattering intensity and minimizing sizing errors that arise from the presence of unwanted scattering modes such as external reflection. For nonabsorbing droplets, forward scattering ($25° < \theta < 45°$) is often preferred to side scattering or backscattering because of the much stronger scattered-light signal. This is especially true in dense sprays, for which attenuation of the probe beams and scattered-light signal can be large and the signal-to-noise ratio is diminished by multiple scattering. In the forward-scattering region, refracted light is used for droplet sizing. The refracted light reaching the receiving optics originates from a very small area on the face of the drop, as illustrated in Fig. 1. All other rays incident upon the droplet are refracted elsewhere; thus it is not necessary to illuminate the entire droplet. In essence, this small area on the droplet surface acts as a lens that magnifies and projects an image of the fringe pattern onto the receiver lens. The resultant magnified fringe spacing is measured as a phase shift between the detectors and, for pure refraction, is linearly proportional to the droplet size. The probe size could theoretically be made as small as or smaller than the size of the projected area on the droplet surface.

The size and shape of the projected area on the surface of the droplet are functions of the receiving optics. The system used in the present study was manufactured by Aerometrics, Inc. The receiver lens was 105 mm in diameter with $f = 5.0$ receiving optics, resulting in a projected area that was approximately 10% of the droplet diameter wide in the scattering plane. The height of the projected area was somewhat less because the light entering the receiving lens was directed to one of three detectors. The shape of the detector apertures was roughly rectangular, with an aspect ratio (width to height) of approximately 2.5 for detectors 1 and 3 and an aspect ratio of 4.5 for detector 2. Therefore the projected area of a 300-μm droplet would be approximately a rectangular area on the front surface of the droplet 30 μm wide in the scattering plane by 12 μm normal to the scattering plane for detector 1.

The detected scattered light from the projected area, also referred to as the interrogation region, will be the average intensity and phase over this region. In theory, the resultant phase should vary only slightly over this region because of the slight change in scattering angle. As the diameter of the probe beams approaches the size of the interrogation region on the droplet surface the resultant intensity will, however, vary significantly as a result of the Gaussian intensity profile of the probe beams. The detected intensity will be proportional to the average incident intensity over the interrogation region. This does not, however pose a fundamental limitation on the minimum usable probe beam diameter.

The minimum usable probe diameter is limited by the droplet transit time and the maximum sampling rate of the instrument. For a discrete Fourier-transform- (DFT-) based signal processor, Ibrahim *et al.*[4] showed that the rms phase measurement error is inversely proportional to the square root of the sample size. At a SNR of 0 dB, the rms phase error for a three-detector configuration was measured to be 1.8° for a sample size of 128. A sample size of 32 would thus have a rms phase error of 3.6°. The signal processor used in this study had a maximum sampling rate of 160 MHz. This would yield a minimum transit time of 0.2 μs for a sample size of 32. The burst detector also requires a finite amount of time in which to trigger the sampling gate. A minimum 16-point DFT burst-detection scheme would require 0.1 μs to trigger the gate on a Doppler burst. Because the burst detector and the signal measurement electronics use an overlapping sampled data set, the burst detector does not increase the signal duration that is necessary for measurement, which will still be 0.2 μs. For a droplet traveling on a trajectory in which the interrogation region would pass through the center of a 60-μm probe diameter, the maximum velocity for size measurement would be 300 m/s. The practical maximum velocity would be somewhat lower for droplets passing through the edge of the probe volume, where the detectable path length would be shorter by a factor of ~2 at the $1/e^2$ probe diameter. Thus the maximum velocity that would provide detectability over the entire beam cross section as defined by D_w for a moderately sized droplet would be 150 m/s, well within the range of most spray applications. Small droplets will have an effective probe diameter smaller than D_w because of limitations on signal triggering within the signal processor and may be detectable only for trajectories through the center of the probe volume, as discussed below.

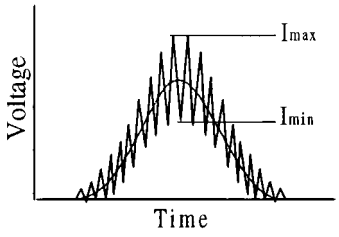

Fig. 2. Typical Doppler burst with a signal visibility of 0.5.

3. Signal Visibility Effects

Another concern when one is measuring droplets that are large with respect to the fringe spacing is signal visibility for the refractively scattered light. A typical Doppler burst signal from a moderately sized droplet with a signal visibility of 0.5 is shown in Fig. 2. The signal visibility (Vis), as defined by

$$\mathrm{Vis} = \frac{I_{\max} - I_{\min}}{I_{\max} + I_{\min}}, \tag{1}$$

is a function of $I_{\max}$ and $I_{\min}$, which are the maximum and minimum amplitudes, respectively, of the raw Doppler burst signal. For small droplets with an interrogation region much smaller than the fringe spacing, the signal visibility will be nearly 1, meaning that the Doppler burst signal will have a maximum amount of signal modulation. This is important because the Doppler burst signal is high-pass filtered in the signal processor to remove the dc pedestal component before sampling. As the droplet size increases and the interrogation region approaches the fringe spacing, the refractive signal visibility approaches zero. The reflective signal visibility, however, will still be large, because the interrogation spot size for reflection is much less than that for refraction. Thus, for a large droplet, even though the absolute magnitude of scattered-light intensity might be much larger for refraction than reflection, the signal modulation that results from the coherent interaction of the two scattering modes will be dominated by reflection. This phenomenon will affect PDI measurements with large probe diameter/droplet size ratios as well as small ratios. It is important that the refractive signal visibility not approach zero over the droplet size range of interest. One can increase refractive signal visibility by decreasing the beam intersection angle, which increases the fringe spacing, or by decreasing the size of the detector aperture in the direction normal to the plane of scattering for standard PDI systems.

4. Temporal Phase Variance

Several theoretical studies have shown that the phase of a scattered-light signal will vary as a function of droplet location along a given trajectory as well as with the location of the trajectory.[5,6] This holds true even for trajectories normal to the scattering plane.[6] As a droplet passes through the probe volume normal to the scattering plane, the location of the interrogation region for refraction ($p = 1$) and reflection ($p = 0$) with respect to the center of the probe volume changes as a function of location along the trajectory. As the location of each of the interrogation regions changes, so does the relative scattering intensity of each scattering component. This results in a phase that changes slightly as the droplet passes through the probe volume. We used the geometric-optics model described in Ref. 2 to study this effect by varying the droplet trajectories within the 10:1 intensity-defined probe volume while calculating the maximum phase variation as the droplets traversed the probe volume. Calculations were performed from $z = 30$ to $z = -30$ μm, where z is the trajectory coordinate normal to the scattering plane.

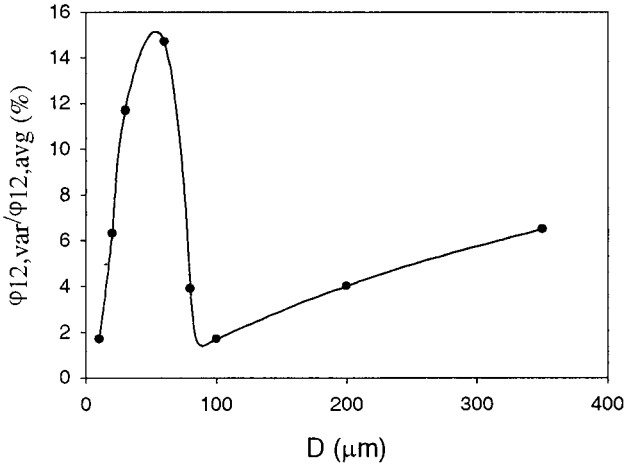

Fig. 3. Maximum phase variance expressed as a percentage of the average phase from detectors 1 and 2 as a function of droplet diameter. Optical configuration of case 1, Table 1.

It was found that the maximum variance in the phase shift always occurred for detectors 1 and 2 and always occurred for trajectories along the edge of the probe volume farthest from the receiver. This is what one might expect, because this is the trajectory where reflective contributions to the total scattered-light signal are maximized. Figure 3 is a plot of the variance in φ_{12} expressed as a percentage of the average φ_{12} as a function of droplet diameter for the optical configuration of case 1 given in Table 1. Droplets much smaller than the probe diameter display little phase variance as a result of the nearly uniform illumination of these small droplets. As droplet size approaches the probe diameter, the relative reflective contribution increases for trajectories along the far edge of the beam waist, which causes an increase in the phase variation as the droplet traverses the probe volume. As the droplet size further increases, the reflective contribution begins to decrease because the reflective and refractive interrogation areas are beginning to separate in space and in intensity. As a result, for droplets much larger than the beam diameter, there are only refractive-dominated or reflective-dominated trajectories. Within the 10:1 intensity range, there are only refractive-dominated trajectories. For droplets

Table 1. Parameters of Optical Configuration for Experiments and Model Calculations

Optical Parameter	Case 1	Case 2
Beam separation (mm)	21	20
Transmitter focal length (mm)	470	500
Receiver focal length (mm)	500	500
Scattering angle (deg)	30	30
Initial beam diameter (mm)	9.6	2.0
$1/e^2$ beam waist diameter (μm)	60	352
Slit width (μm)	50	100
Receiver magnification	2.0	2.0
Receiver lens diameter (mm)	105	105
Laser wavelength (nm)	514.5	514.5
Fringe spacing (μm)	11.52	12.87
S_{12} (mm)	23.34	23.34
S_{13} (mm)	69.00	69.00
S_{13}/S_{12} (mm)	2.96	2.96
Sample rate (MHz)	160	40
Sample size	64	64

larger than ~100 μm there is again an increase in phase variance, probably as a result of the large variation in illumination intensity over the refractive interrogation region, which is approaching the beam waist diameter.

The effect of phase variance on the response of the instrument is strongly dependent on the duration of the sampled Doppler burst and the droplet velocity. For a minimum sample time of 0.2 μs and a droplet velocity of 150 m/s, the maximum sampled path length would be 30 μm, which is less than the 60-μm path length shown in Fig. 3. Inasmuch as the phase variance is fairly linear with path length, the maximum variation in φ_{12} for a 60-μm droplet would be (30 μm/60 μm) $\times$ 15%, which is equal to 7.5%. This small variation in phase over the sampled burst would slightly decrease the SNR of the Fourier-transformed signal but would not cause a substantial measurement error.

5. Probe Volume Correction

A. Conventional Probe Volume Correction

It is well known that the cross-sectional area of the probe volume varies with the particle diameter that is being measured.[7] This is due to the nature of the Gaussian intensity distribution at the probe volume and the fact that droplets much larger than the wavelength of light scatter light in proportion to the square of the droplet diameter. Larger particles will scatter more light and therefore be detected farther away from the center of the probe volume than will smaller particles. A correction factor, commonly referred to as the probe volume correction (PVC), is usually employed in commercial signal-processing software and takes this into account. The software used in this study offered a PVC based on either an analytical correction or a transit time correction that measures the maximum path length for each particle size class and assumes that this length is equal to the maximum probe diameter for that size class. The corrected number of counts in each size class is calculated as

$$n_c(D) = n(D)\left[\frac{L_{\max}}{L(D)}\right], \tag{2}$$

where $L_{\max}$ is the maximum path length through the probe volume, which occurs for the largest droplet size class, and $L(D)$ is the measured maximum path length for each size class.[8] This PVC does not, however, take into account the decrease in the width of the probe volume when intensity validation is used to clip the edges of the probe volume to eliminate trajectory-dependent scattering errors. A new PVC based on the estimated diameter of the probe volume for each size class at the minimum intensity cutoff is therefore needed.

B. Signal Dynamic Range and Intensity-Based Probe Volume Correction

In a typical spray, the range of measured droplet sizes can be quite large. The PDI instrument used in this study was capable of sizing droplets over a dynamic size range of 50:1, with the limit being the dynamic range of the photomultiplier tubes (PMT's) and detection electronics. The dynamic range is bounded by signal saturation on the PMT's and the minimum signal that can be measured at a fixed SNR. Ibrahim *et al.*[4] have shown that a DFT-based signal processor is capable of making reliable phase measurements at a SNR as low as -10 dB. The use of a 10:1 intensity-validation criterion within each size class would produce an intensity dynamic range of 25,000:1. The signal processor used here was capable only of measuring a scattered-light intensity range of 1,000:1.

One can overcome the dynamic range limitation by setting the maximum intensity of a droplet as one third of the maximum measurable droplet size to just saturate the detector, I_{sat}. For the optical configuration of case 1 in Table 1 and a droplet size range of 50:1, the maximum droplet size, $D_{\max}$, is 310 μm for water droplets in air. Droplets larger than $D_{\max}/3$ will tend to saturate the instrument, with a droplet of diameter $D_{\max}$ having a theoretical maximum scattering intensity of $9I_{\text{sat}}$. It is important that we know not the intensity of these larger droplets but that their scattering intensity is above $0.9I_{\text{sat}}$, which is the 10:1 lower intensity cutoff for this size class. It should be pointed out that, although signal saturation does degrade the SNR, the affect on phase measurement accuracy is minimal because of the strong signal and thus the high SNR.

The smallest measurable droplet size of $D_{\max}/50$ (for a 50:1 size range) would yield a maximum scattering intensity of $3^2(1/50)^2I_{\max}$. For the signal processor used here, the minimum measurable signal was ~0.5 mV, but the minimum signal required to produce an instrument trigger was 1 mV. For droplet sizes with a signal less than 1 mV within the probe volume defined by a 10:1 intensity range, a correction

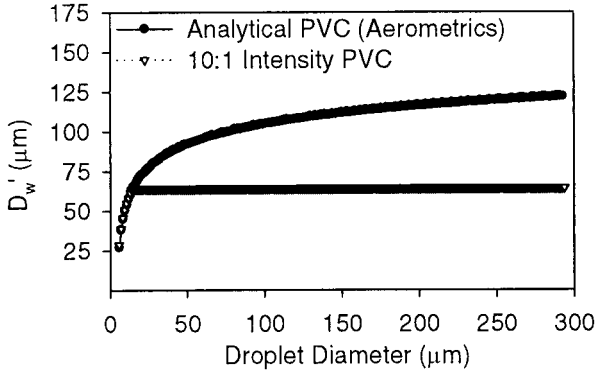

Fig. 4. Calculated probe diameter (D_w') versus droplet diameter; analytical PVC and 10:1 intensity PVC.

factor must be employed that accounts for the reduced probe cross-sectional area over which measurements may be made. For the optical configuration studied here, a 14.6-μm droplet would produce a maximum scattering intensity of 10 mV for an I_{sat} of 500 mV. For droplets in the size range of 6.2–14.6 μm, a probe volume correction factor must be employed. The diameter of the probe volume for droplets in this size range is simply the diameter of the Gaussian probe beam at which the scattering intensity equals 1 mV.

Assuming a Gaussian intensity distribution in the probe volume, the width of the beam waist at the lower cutoff point (D_w') can be calculated. The Gaussian intensity distribution at the beam waist is given by

$$\frac{I}{I_0} = \exp\left(\frac{-8y'^2}{D_w^2}\right), \tag{3}$$

where I_0 is the intensity at the center of the beam waist and y' is the distance from the center normal to the beam propagation direction. For the present optical configuration (case 1, Table 1), $D_{w10\%} = 64$ μm. With a 14.6-μm droplet producing a peak scattering intensity of 10 mV, the probe diameter at the 1-mV detection limit would be

$$\begin{aligned} D_w' &= \left\{\frac{-D_w^2}{2}\ln\left[\frac{(D_{\max}/3)^2}{D^2 I_{\text{sat}}}\right]\right\}^{1/2} \\ &= \left[\frac{-D_w^2}{2}\ln\left(\frac{21.32}{D^2}\right)\right]^{1/2}, \qquad D < 14.6\ \mu\text{m}. \end{aligned} \tag{4}$$

For droplets larger than 14.6 μm, D_w' is fixed at 64 μm. A plot of the probe diameter calculated from the intensity cutoff scheme [Eq. (4)] and the currently employed analytical PVC from the commercial software used here is shown in Fig. 4. The intensity-based probe volume is constant at 64 μm for droplets from 14.6 to 310 μm. For droplets smaller than 14.6 μm, Eq. (4) is used. The analytical PVC currently employed in the commercial software has a probe diameter that continuously increases with droplet size.

6. Implementation of Intensity Validation

The intensity-validation technique can be implemented by setting of the maximum intensity to be at saturation, I_{sat}, for a droplet size equal to one third of the maximum measurable size $D_{\max}$. The maximum intensity line then follows an $I \propto D^2$ relationship for the other droplet size classes.

For the measurements presented here, the PMT voltage was set above 400 V to ensure that the PMT's would respond linearly with scattered-light intensity. Linearity was verified experimentally with a monodispersed droplet experiment. The signal-processing software employed an intensity-validation setup page in which data were collected and a plot of diameter versus the square root of intensity was displayed. Laser power or PMT voltage was then adjusted until the maximum intensity reading in each size class fell upon the upper intensity cutoff line. Data were then collected and postprocessed to reject particles in each size class with an intensity less than 10% of the maximum intensity within that size class. The PVC described above was employed to account for the smaller probe diameter for droplets less than 14.6 μm in diameter.

The probe cross-sectional area described in Eq. (5) is a parallelogram defined by the receiver slit and probe diameter as given in Fig. 4:

$$A = \frac{D_w' D_s}{\sin(\theta)}. \tag{5}$$

Inasmuch as the receiver is imaging only a small spot on the droplet surface, droplets are essentially treated as point sources of mass passing through the probe cross section. This allows a droplet much larger than the probe cross section, along with all the droplet mass flux, to be counted as being entirely within the probe area. In a spray where the droplet trajectories are generally Poisson distributed there will also be instances in which the interrogation region passes outside the probe cross section and is not measured, yet some of the droplet does pass through the probe. As long as enough droplets are sampled in a spray (typically >5000) the stochastic nature of the trajectories will ensure that these sampling cross-sectional variations are averaged out, so Eq. (5) does indeed represent the true probe cross-sectional area for mass flux calculations.

The corrected number of counts for each size class is given by

$$n_c(D) = n(D)\left(\frac{A_{D_{w10\%}}}{A}\right), \tag{6}$$

where $A_{D_{w10\%}}$ is the probe area calculated with the beam waist diameter (64 μm) at the lower-intensity cutoff for droplets larger than 14.6 μm in diameter. The technique of monitoring the scattered light intensity and adjusting PMT voltage or laser power is

necessary because light extinction caused by spray attenuation and window reflections can cause the absolute scattered light intensity to vary. The intensity-validation scheme, however, relies not on absolute scattering intensity but only on scattering intensity relative to the maximum measured intensity within each size class.

Another benefit of this technique is that it provides a tractable method for setting the PMT voltage and laser power. Several studies have shown a sensitivity of the measurement to the PMT voltage setting at a given laser power.[7,9] The informational feedback of the intensity-validation method allows the user of the instrument to preselect an upper intensity-versus-diameter relationship and set the PMT voltage to match that relationship.

The intensity-validation scheme described herein was calculated for a particular size range corresponding to the optical configuration used in this study. A similar PVC could be generated for any size range of 50:1 or less, as long as the saturation point is set for a droplet that is one third of the maximum measurable droplet size. Also, it is not necessary that the response of the detector be linear with scattered light intensity. As long as the instrument response is known, the linearized intensity can be calculated and used in the intensity-validation scheme. In fact, a nonlinear detector could be used to increase the dynamic range of measurable droplet sizes.

7. Spray Measurements

Using the 10:1 intensity-validation scheme and associated PVC, we performed measurements with a dilute water spray to demonstrate the technique. The PDI instrument used in this study was the same as described in Ref. 2. The spray came from a Delavan WDB 10-45° nozzle operated at 0.34 MPa and at atmospheric backpressure. Measurements of droplet size, velocity, and volume flux were made as a function of radial position in the spray at a location of 10 cm downstream of the injection point. Measurements were made with both the current small probe volume configuration (case 1, Table 1) and a more conventional probe volume (case 2, Table 1), with and without intensity validation. Measurements of volume flux are presented in Fig. 5 along with the volume flux measured with a collection tube. We assessed the accuracy of the collection tube measurement by integrating the radial flux profile and comparing it with the measured injected flow rate. The integrated collection tube measurement was 8% lower than the measured injected flow rate. As can be seen from the figure, without intensity validation the PDI measured volume flux is much larger than the collection tube measurement, even with the larger probe volume. This is a result of small particles' passing through the edges of the probe volume and being erroneously measured as much larger particles, thus greatly adding to the measured volume flux. Good agreement between the collection-tube-measured volume flux and the volume flux measured with the small probe volume and 10:1 intensity-validation scheme can be seen in Fig. 5. These experiments were conducted before the detector separation ratio was changed to a noninteger number ($S_{13}/S_{12} = 2.96$), which would allow droplets larger than 150 μm to be measured as smaller droplets. The maximum valid droplet size was just under 150 μm for this particular spray, and intensity validation alone was sufficient to permit rejection of erroneous measurements.

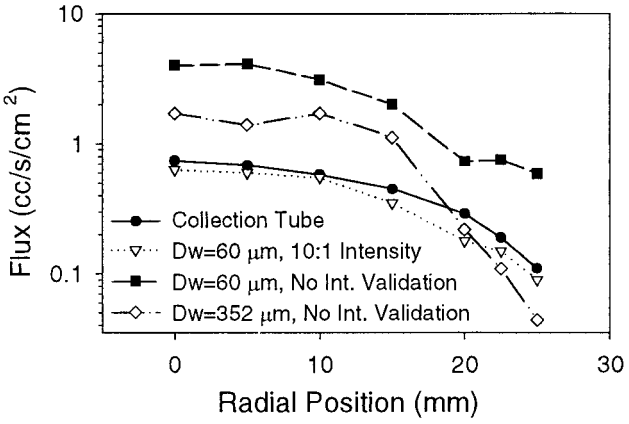

Fig. 5. Volume flux versus radial position. Delavan WDB 10-45° nozzle, $P = 0.34$ MPa, $Z = 10$ cm.

Figure 6 shows a scatter-plot droplet diameter versus the square root of the scattered light intensity for a radial position of 0.0 mm. Also shown are the high- and low-intensity lines. The suspect particles are those larger than ~150 μm, which show only low scattering intensities. Figure 6 also reveals another important advantage of using intensity validation, which is the ability to detect multiple-droplet occurrences in the probe volume. For single-droplet occurrences, a sharp cutoff in the data near the maximum scattering line would be observed, as in Fig. 6. Because two or more droplets coincident in the probe volume would scatter significantly more light, multiple-droplet occurrences would show up as

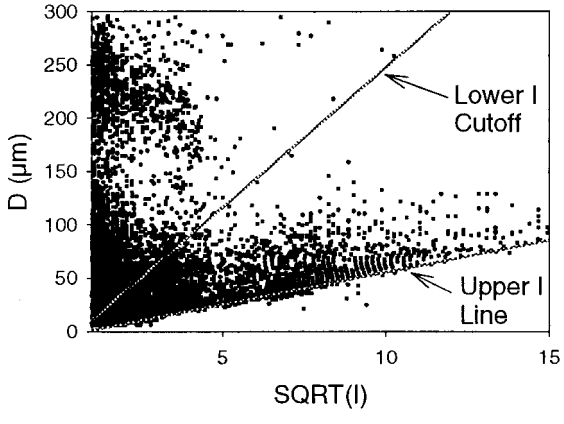

Fig. 6. Scatter plot of droplet diameter versus square root of intensity. Delavan WDB 10-45° nozzle, $P = 0.34$ MPa, $Z = 10$ cm, $r = 0.0$ mm.

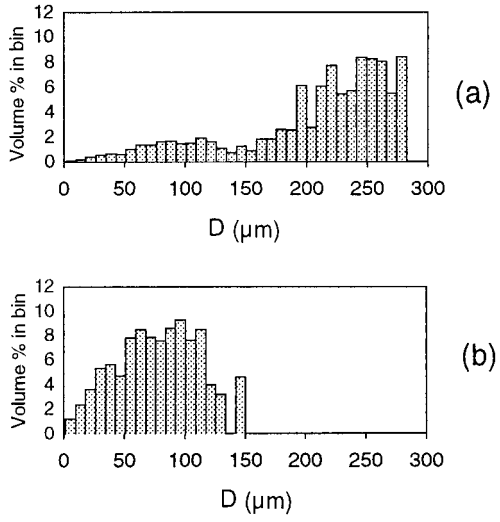

Fig. 7. Histograms of relative volume percentage. Delavan WDB 10-45° nozzle, $P = 0.34$ MPa, $Z = 10$ cm, $r = 0.0$ mm; (a) without intensity validation, (b) with intensity validation.

scattering in the data at intensities greater than the upper intensity line.

Figure 7 is a histogram of the relative volume concentration for the radial location of 0.0 mm with and without intensity validation, demonstrating the significant change in volume distribution in a real spray when trajectory-dependent errors are eliminated. It is interesting that even with a maximum droplet size of 150 μm, the mass flux measured with the 352-μm probe diameter (Fig. 5) was still significantly greater than the mass flux measured with the collection tube. This could be a result of the slit effect discussed in Ref. 2, which showed an increase in the number of measurement errors when the slit was accounted for with the larger beam waist diameter.

8. Conclusions

Although there are certain practical limitations on minimum usable probe diameter, current DFT-based signal processors are quite capable of making accurate droplet-size measurements for relatively small probe diameters and high flow velocities. Optical limitations such as on signal visibility can be overcome by proper selection of the beam crossing angle or detector aperture. Droplets much larger than the beam waist can be measured when a combination of phase-ratio and intensity-based validation criteria are used. An intensity-based probe volume correction factor has also been shown to provide a simple and robust way to calculate the probe cross-sectional area. The implementation of the technique also provides a tractable method for determining the appropriate laser power and PMT voltage during an experiment. Measurements in dilute sprays have demonstrated that the technique is capable of rejecting trajectory-dependent scattering errors while greatly improving the accuracy of liquid flux measurements.

Appendix A. Nomenclature

A	Probe cross-sectional area (μm^2)
C	Number of counts
C_c	Corrected number of counts
D	Droplet diameter (μm)
D_{max}	Maximum measurable droplet size (μm)
D_s	Apparent slit width (μm)
D_w	$1/e^2$ beam waist diameter (μm)
$D_{w10\%}$	Probe diameter at 10% of I_{max} (μm)
D_w'	Probe diameter (μm)
I	Intensity (W)
I_0	Intensity at beam center (W)
I_{max}	Maximum signal intensity (mV)
I_{min}	Minimum signal intensity (mV)
L_{max}	Maximum path length (μm)
I_{sat}	Saturation intensity (mV)
$L(D)$	Path length (μm)
N	Droplet number density (cm^{-3})
y'	Distance from center of beam waist (μm)
φ	Phase difference (deg)
θ	Scattering angle (deg)
Subscript 12	Detectors 1 and 2

The authors thank Mike Griggs for his assistance in operating the facility and conducting experiments.

References

1. S. V. Sankar and W. D. Bachalo, "Performance analysis of various phase Doppler systems," presented at the Fourth International Congress on Optical Particle Sizing, Nuremberg, Germany, 21–23 March 1995.
2. P. A. Strakey, D. G. Talley, S. V. Sankar, and W. D. Bachalo, "Phase-Doppler interferometry with probe-to-droplet size ratios less than unity. I. Trajectory errors," Appl. Opt. **39,** 3873–3884 (2000).
3. P. Haugen, E. I. Hayes, and H.-H. von Benzon, "Size and velocity measurements of large drops in air and in a liquid–liquid two-phase flow by the phase-Doppler technique," Part. Part. Syst. Charact. **11,** 63–72 (1994).
4. K. M. Ibrahim, G. D. Werthimer, and W. D. Bachalo, "Signal processing considerations for laser Doppler and phase Doppler applications," presented at the Fifth International Symposium on the Application of Laser Techniques of Fluid Mechanics, Lisbon, Portugal, 9–12 July 1990.
5. Y. Hardalupus and C. H. Liu, "Implications of the Gaussian intensity distribution of laser beams on the performance of the phase Doppler technique. Sizing uncertainties," Prog. Energy Combust. Sci. **23,** 41–63 (1997).
6. G. Grehan, G. Gouesbet, A. Naqwi, and F. Durst, "Trajectory ambiguities in phase Doppler systems: study of a near-forward and near-backward geometry," Part. Part. Syst. Charact. **11,** 133–144 (1994).
7. W. D. Bachalo, R. C. Rudoff, and A. Brena de la Rosa, "Mass flux measurements of a high number density spray system using the phase Doppler particle analyzer," paper AIAA 88-0236, presented at the Twenty-Sixth Aerospace Sciences Meeting, Reno, Nev., 11–14 January 1988.
8. Aerometrics Phase Doppler Particle Analyzer Doppler Signal Analyzer, 1-Component User's Manual, Release 1.0, April (Aerometrics Inc., Sunnyvale, Calif., 1993), App. B.
9. C.-P. Mao, "Measurements of sprays using phase Doppler instruments: a study to establish formal operating procedures," presented at the Ninth Annual Conference on Liquid Atomization and Spray Systems, San Francisco, Calif., 19–22 May 1996.